Advances in Computational Design, *Vol. 4, No. 4 (2019) 343-365*
DOI: https://doi.org/10.12989/acd.2019.4.4.343

A new design method for site-joints of the tower crane mast by non-linear FEM analysis

Yoshitaka Ushio*[1], Tomoharu Saruwatari[2a] and Yasuyuki Nagano**[1]

[1]*Graduate School of Simulation Studies, University of Hyogo 7-1-28 Minatojima-Minamicho, Chuo-ku, Kobe 650-0047, Japan*
[2]*Engineering Technology Div. JSOL Corporation 2-2-4 Tosabori, Nishi-ku, Osaka, 550-0001, Japan*

(Received September 21, 2018, Revised March 28, 2019, Accepted April 30, 2019)

Abstract. Among the themes related to earthquake countermeasures at construction sites, those for tower cranes are particularly important. An accident involving the collapse of a crane during the construction of a skyscraper has serious consequences, such as human injury or death, enormous repair costs, and significant delays in construction. One of the causes of deadly tower crane collapses is the destruction of the site joints of the tower crane mast. This paper proposes a new design method by static elastoplastic finite element analysis using a supercomputer for the design of the end plate–type tensile bolted joints, which are generally applied to the site joints of a tower crane mast. This new design method not only enables highly accurate and reliable joint design but also allows for a design that considers construction conditions, such as the introduction of a pre-tension axial force on the bolts. By applying this new design method, the earthquake resistance of tower cranes will undoubtedly be improved.

Keywords: computer simulation, tower crane, FEM, bolted tensile joints, joint design

1. Introduction

Among the themes related to earthquake countermeasures at construction sites, those for tower cranes are particularly important. An accident involving the collapse of a crane during the construction of a high-rise building has serious consequences, such as human injury or death, enormous repair costs, and significant delays in construction. However, given that a tower crane is a temporary structure, the cost and time effectiveness are often emphasized over safety.

The mast structure is critical for the earthquake resistance of tower cranes. In particular, the site joints of the mast are very critical structural system. There was a typical example of an earthquake-related tower crane accident during the construction of a high-rise building in Taiwan, where the one of the authors, Yoshitaka Ushio, was in charge of the site work as the project director. In this accident, the endplate-type tensile bolted joints of the tower crane mast collapsed. In order to prevent such an accident, attention should be paid to the structural design of tower crane mast

* Corresponding author, Student (Ph.D. course), E-mail: ymmushio@gmail.com
**Corresponding author, Professor, E-mail: nagano@sim.u-hyogo.ac.jp
[a] Manager, E-mail: saruwatari.tom@jsol.co.jp

http://www.techno-press.org/?journal=acd&subpage=7 ISSN: 2383-8477 (Print), 2466-0523 (Online)

joints. Therefore, this study focuses on the design of site bolt joints of tower crane masts and proposes a new simulation-based design method. Specifically, a design method/procedure with static elastoplastic FEM analysis using a supercomputer is proposed. This method is based on the current allowable stress design criteria for end plate–type bolted tensile joints joining a tower crane mast blocks on site.

Although many papers on FEM elastoplastic analysis of end plate-type tensile bolted joints have been published in the past, their contents are to prove the validity of the proposed design formula or to study the mechanical behavior and performance of the joints, etc. On the other hand, this paper proposes a design method/procedure for site joints of tower crane masts (end-plate type tensile bolted joints) that directly use the results obtained by using a supercomputer and LS-DYNA, which is the software for FEM elastoplastic analysis. In this analysis, in order to maximize the reproducibility, based on the performance of the computer, a model comprising minimal hexahedrons elements of 2.5 mm on each side was adopted to obtain more accurate design.

2. Overview of the effects of seismic damages on tower cranes

During a high-rise building construction in Taiwan approximately 15 years ago, an earthquake caused a catastrophic disaster in which two tower cranes collapsed from a height of 250 m because of the breakage of their mast bolt joints (Loh et al. 2003; Ushio et al. 2017). Owing to this disaster, this project suffered great damage, including deaths, injuries, and damage to the building itself.

On the contrary, a number of collapse-and-fall accidents of tower cranes at construction sites were reported after the Hyogo-ken Nanbu (Japan) earthquake, which occurred in January 1995. However, there was no human injury because the earthquake occurred in the early morning hours. Although the infrastructure damage was massive, this story was not largely reported by the media. The Department of Labor (now the Ministry of Health, Labor, and Welfare) performed a field survey with the Japan Crane Association to understand the extent of damage to the cranes and develop countermeasures for prevention. In response to this, research on the seismic design of cranes began in Japan. Regarding the survey results of Takanashi (2005), the number of cranes damaged is shown in Fig. 1(a) by type. There are many cases of damage to tower cranes, and the destruction situation (Fig. 1(b)) accounts for 38 percent of fatal damage, such as the breakage of the mast and foundation. It can be imagined that human casualties would have been significant if the earthquake had occurred during the day.

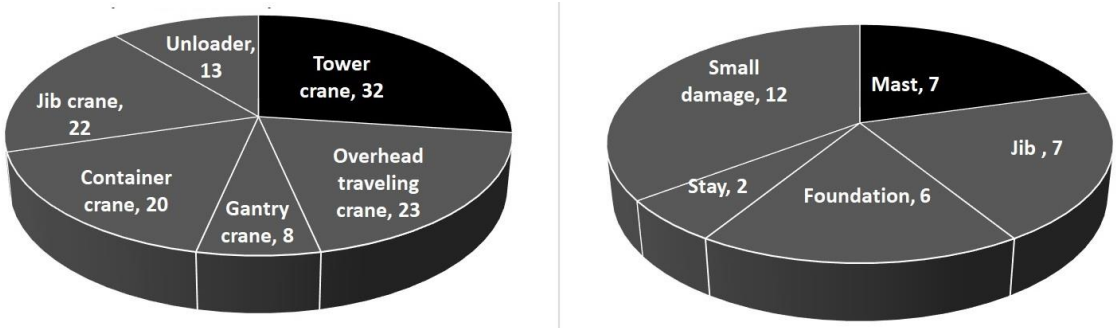

(a) Type of cranes damaged (Number of cranes)

(b) Parts of tower cranes damaged (number of cranes)

Fig. 1 Damage to cranes after the Hyogo-ken Nanbu earthquake

Fig. 2 Destruction of a tower crane mast of a high-rise in Taiwan

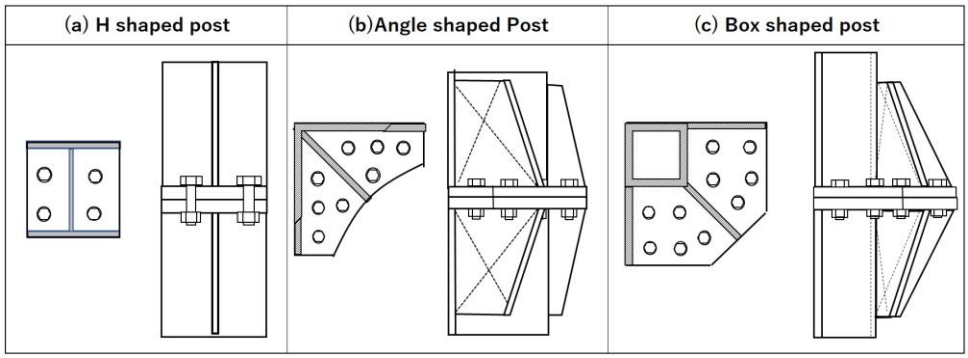

Fig. 3 Typical site joints of a tower crane mast

Figure 2 shows the abovementioned destruction of the tower crane mast, which occurred during the construction of the high-rises in Taiwan. It also shows that the tower cranes were collapsing because of the destruction of the bolts at the field bolt joints. The sudden collapse of the crane caused by the destruction of these bolts resulted in an evacuation problem for tower crane operators and in the expansion of the damages caused by the collapse of a crane. Similar cases were also reported after the Hyogo-ken Nanbu earthquake.

For tower crane mast joints, the problem is that the design conditions of the joints are more severe because the outer surface of the mast needs to be flat for climbing the tower crane. Depending on the shapes of the post members of the mast, large-diameter bolted joints (greater than 30 mm), eccentric-bolted tension joints, etc., are applied for site joints (Fig. 3). In the case of the abovementioned Taiwan high-rises, large-diameter (e.g. 45 mm diameter) high-strength bolts were used for the joints. For the post members of tower cranes in Japan, rectangular shape steel tubes are normally used for large cranes, and angle-shaped steel are used for small cranes; thus, many eccentric bolt tensile joints, such as (b) and (c), are observed. The use of H-shaped steel posts (a) was adopted for the tower crane that collapsed in the Taiwan high-rise during the earthquake.

3. Outline of the joint design

3.1 Two design methods for end plate–type tensile bolted joints

Figure 4 shows the design flow diagram for the end plate–type bolted tensile joint. The blue

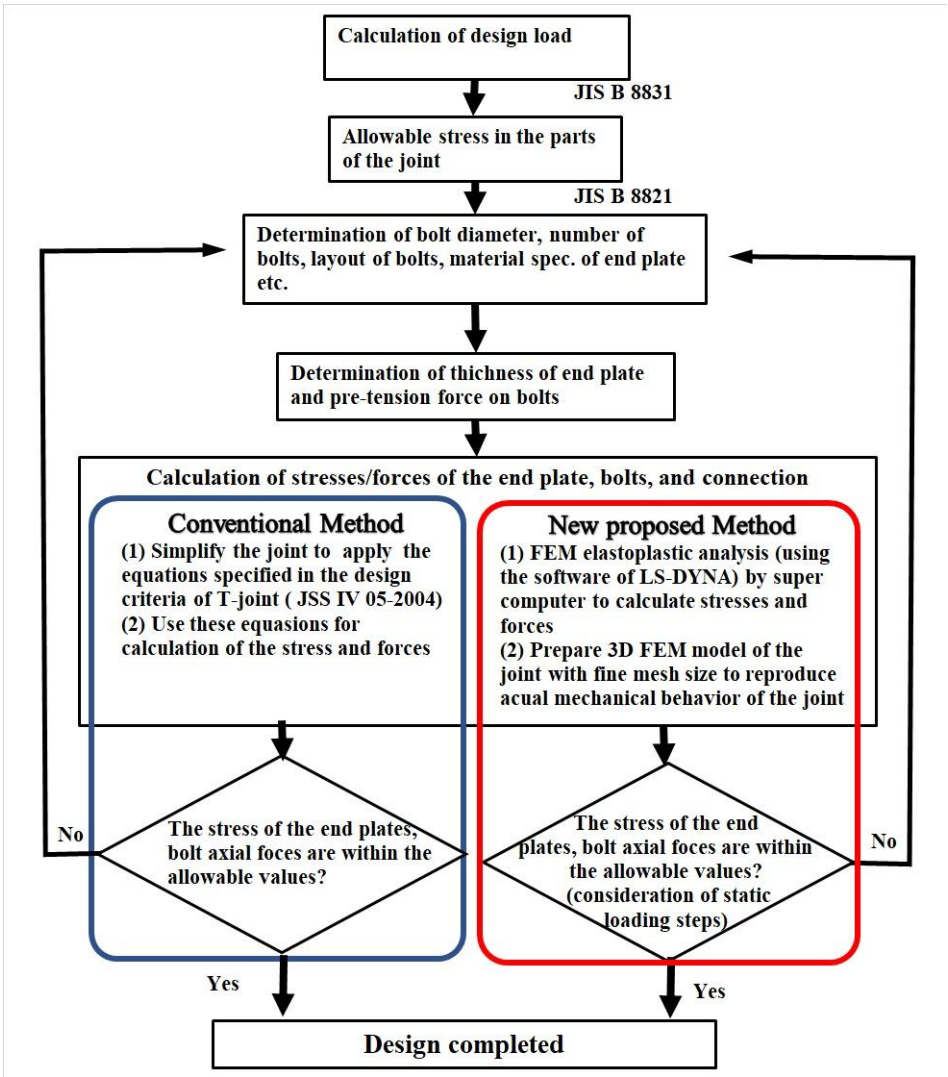

Fig. 4 Joint design flow of the conventional and new design method

frame and red frame represent the conventional method and the design procedure proposed in this paper respectively.

High-strength tensile bolted joints have been studied by many researchers on a design method for the T-joint (split tee types and endplate types) described in JSS IV 05-2004. There are still many studies on this subject such as by Yang et al. (2013) and by Wang et al. (2015). Given the complicated mechanical properties of this joint type owing to the effect of the prying action force caused by the rigidity of the end plate, arrangement of the bolts and pre-tensioned axial forces on the bolts, there are some problems with the design method. To understand these mechanical properties and devise a design formula, a method of confirmation by experiments was used. However, the use of this approach to create an accurate design formula for all types of joints would be costly and time consuming. Therefore, the details of joints are often simplified such that the

Table 1 Advantages and disadvantages of the two design methods

Item	Conventional	Proposed
(1) Applicable to all types of joints (see Figs. 1–3)		✓
(2) Accurate calculation of stresses and forces on joint parts		✓
(3) Accurate calculation of the effects of the prying action to the stresses and forces on the joint parts		✓
(4) Accurate calculation of the effects of the pre-tension force of the bolts to the stresses and forces on the joint parts		✓
(5) Calculation time and cost	✓	

design formula can be universally applied to the design of a joint. Herein, this method is referred to as the "conventional design method."

In contrast, with advances in analysis software and improvements in the calculation speed of supercomputers, structures can be accurately and easily reproduced along with their dynamic behavior via computer simulations. This approach would allow the accurate creation of a design for all types of joints. Furthermore, if it is applied to the in-situ fitting of a tower crane mast, it will provide us with a structural system and design method that is safe, cost efficient and workable. This forms the basis of the proposed new design method.

Table 1 lists the advantages and disadvantages of the abovementioned design methods. Herein, the author uses the mast joint of the tower crane of which details and capacity are the same as those of the tower crane that collapsed in the earthquake during the construction of the aforementioned high-rise in Taiwan.

3.2 Design load calculation

The Japanese seismic design standards for tower cranes are specified in JIS B 8821 (2013) and JIS B 8831 (2004).

Regarding earthquake loads, the standard specifies that "to apply a horizontal load that is 20 percent of its own weight, regardless of whether it is the traveling type or fixed type, but not to consider the seismic horizontal load of the weight suspended by rope, but in case that dynamic analysis of the structure against an earthquake is done, this condition need not be applied." In this standard, the seismic load is taken into consideration in load combination C (hoisting load + self-weight load + seismic load + heat load) out of load combinations A, B, and C. Considering that load combination C is the most critical for the structural design of this type of tower crane, the stresses and forces on the structural members calculated under that combination are compared with the allowable stresses.

For the calculation of the design load acting on the site joint portion of the tower crane mast, a 3D truss of the mast structure is analyzed by the application of the load of condition C, including the seismic load specified in JIS B 8831 (2004). By assuming the load combination of a tower crane of 500 tm (25 t × 20 m) capacity (similar to the one that collapsed during the earthquake in Taiwan), the forces applied to the mast members are calculated, and the maximum tensile force on the post member is found to be 2148 kN. Meanwhile, the tensile force acting on one bolt is 537 kN. Furthermore, the sizes of the mast frame members are designed on the basis of member stresses calculated under the condition of this designed load. The calculation of the design load in load combination C is shown in Fig. 5.

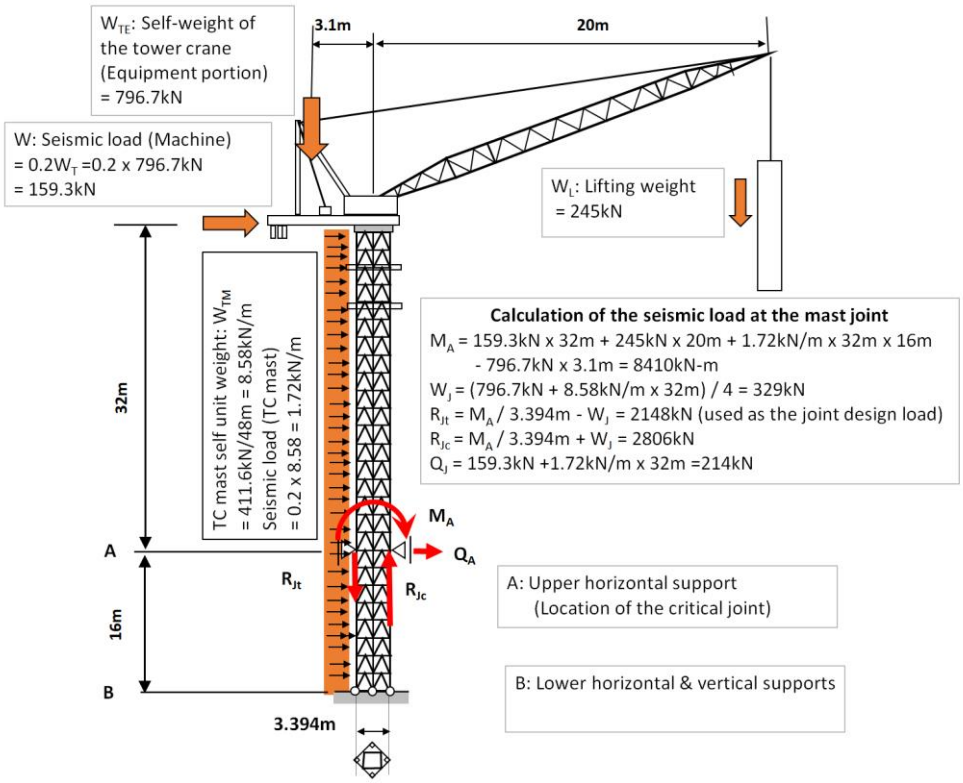

Fig. 5 Loading condition with seismic loading for the design of the crane structure

For the design load on the joint, only a tensile load of 537kN per mast post was considered, because the shear load is small and can be resisted by the friction between the end-plates.

JIS B 8831 (2004) specifies that the value of the seismic load shall be the load equivalent to 20% of the vertical static load on the crane. A tower crane is defined as being a temporary structure (short installation duration); therefore, construction costs and work efficiency constitute a greater concern. In the standard defining the earthquake resistance of a tower crane, the applied safety factor is lower than that for permanent buildings. However, considering the seriousness of the damage that could be caused by an earthquake disaster involving a tower crane, Takanashi (2007) indicated that the design acceleration specified by the seismic design standard for cranes is insufficient for those cases in which a crane connected to a building is influenced by the seismic response of that building as well as the ground characteristics (seismic wave characteristics). In response, JCAS 1101 (2008), a seismic design guideline for cranes, was issued, and a new design seismic load and design method for overcoming these problems were proposed. Recently, the new standard ISO11031 (2016) standard on seismic design of cranes was approved by the related member countries in 2016, and there is a possibility that future seismic design standards in Japan such as JCAS 1101 (2008) may be updated to reflect this ISO11031(2016) as described by Kobayashi (2017).

However, as for earthquake-resistant design loads, the value calculated on the basis of JIS B 8831 (2004) was adopted herein because this study focuses on the design method.

Table 2 Strength factors

Load Combination	Strength Factor	
	For Yield Point	For Tensile Strength
Load combination A	1.5	1.8
Load combination B	Value for load combination A divided by 1.15	Value for load combination A divided by 1.15
Load combination C	Value for load combination A divided by 1.3	Value for load combination A divided by 1.3

3.3 Allowable stresses in joint parts for tower crane mast design

The allowable stresses for the structural design of tower cranes are given by the safety factor method and specified in JIS B 8821 (2013): "The basic allowable stress σ_a shall be the smaller value of either the yield point (or 0.2% strain yield strength) or tensile strength of the material divided by the strength factor given in Table 2 for each load combination given in JIS B8831 (2004)."

- The yield point of the end plate σ_y = 340 N/mm^2 and the tensile strength σ_u = 500 N/mm^2
- The yield point of bolts σ_{By} = 900 N/mm^2 and tensile strength σ_{Bu} = 1000 N/mm

Therefore, the allowable stress σ_{Ba} in the bolt and the allowable stress σ_a in the end plate are determined as follows based on the JIS standard

$$\sigma_a = \sigma_y/(1.5/1.3) = 340/1.154 = 295 \text{ N/mm}^2 \quad (1)$$

$$\sigma_{Ba} = \sigma_{Bu}/(1.8/1.3) = 1000/1.385 = 722.0 \text{ N/mm}^2 < \sigma_{By}/(1.5/1.3) = 779.9 \text{ N/mm}^2 \quad (2)$$

According to JIS B 1082 (2009), the effective cross-sectional area of the bolt is A_{se} = 1306 mm^2 in the case of M45 bolts. Therefore, the allowable axial force on M45 bolts is 943 kN.

3.4 Determination of diameter, strength, and number of bolts in the joint

The diameter, strength, and number of bolts are first determined temporarily so that the total tolerable bolt tensile strength of the joint is greater than the allowable tensile strength of the post member of the tower crane mast. In this case, four M45 hexagon bolts of strength class 10.9 are taken. Depending on the analysis results, this content may be changed if necessary.

- The allowable tensile strength of four bolts = 4 × 1000 (Nmm^2) / 1.385 × 1306 mm^2/1,000 = 3772 kN
- The allowable tensile strength of an H-shaped steel post = 340 (N/mm^2) / 1.154 × 11800 mm^2 = 3477 kN

4. Conventional method for the end plate–type tensile bolted joint design

4.1 Application of design criteria JSS IV 05-2004

Regarding the design criteria for high-strength bolted tensile joints, given that there is no

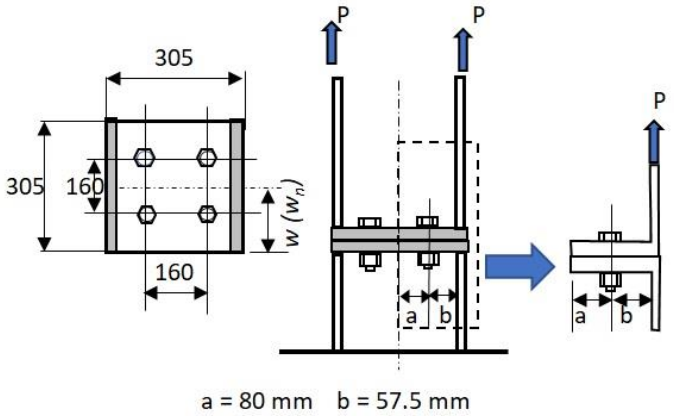

Fig. 6 Modeling of the joint for design

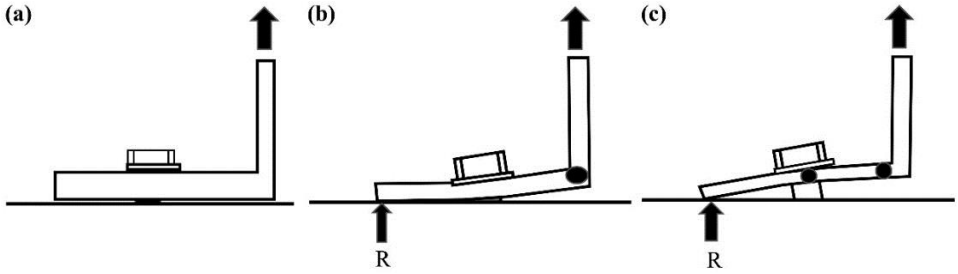

Fig. 7 Behavior of a T-joint depending on flange thickness (JSS IV 05-2004)

provision concerning the design method in the abovementioned JIS B8821 (2013), the design criteria for T-joints specified in JSS IV 05-2004 are determined suitable for the design of this type of joint.

To use these criteria, this tower crane mast joint is simplified as one in which the web portion of the H-shaped steel post is ignored and all tensile forces act only on the flanges (Fig. 6). Consequently, the design criteria for a T-joint may be applied to the bolted tension joint of a tower crane mast post that is made of H-shaped steel. In consideration of the prying action of the joint, the bolt tensile force and end plate bending stress can be calculated.

4.2 Design of T-joints according to the design criteria in JSSIVJSS IV 05-2004

4.2.1 Basic concept of the design criteria in JSS IV 05-2004

According to these criteria, the design and checking of a T-joint should be performed in consideration of the fact that the joint behavior depends on its flange thickness. When a tensile force acts on a T-joint, the joint behaves differently depending on the size of the T-flange thickness, and the limit states reaching the allowable stress level are generally classified into three types (Fig. 7). Thereafter, the design and checking should be performed for each state.

(a) The case in which a T-flange is thick and the bolt stress reaches its allowable stress before the T-flange

(b) The case in which the T-flange thickness is between (a) and (c) and both the bolt stress and T-flange stress reach an allowable level

(c) The case in which the T-flange is thin and reaches its allowable stress before the bolt

4.2.2 Checking the axial force on the bolts (the parameters are listed in the Appendix)

(1) When the work force P is a tensile force, the axial force B per bolt is obtained using Eq. (3) or (4)

$$B = B_0 (1 + p), \quad where \qquad P < B_0 \tag{3}$$

$$B = P (1 + p), \quad where \qquad P \geqq B_0 \tag{4}$$

(2) The axial force per bolt that becomes the maximum will satisfy Eq. (5):

$$\frac{B}{A_{se}} \leq \sigma_{Ba} \tag{5}$$

In these equations, p is the prying action force coefficient, which can be obtained from the following equations:

(1) $P \geq B_0$,

$$p = \{0.7845 - 0.1278(w/120)\} - [\{-0.1991 + 0.3644(w/120)\} + \{0.0130 - 0.0076(w/120)\}t](P/B_0), \tag{6}$$

(2) $P < B_0$,

$$p = [\{1.6949 - 4.4147(w/120) + 3.1598(w/120)^2\}(t/d)^3 + \{-8.2310 + 21.1358(w/120) - 15.2549(w/120)^2\}(t/d)^2 + \{13.0538 - 33.4313(w/120) + 24.3475(w/120)^2\}(t/d) + \{-5.8936 + 16.4708(w/120) - 12.1872(w/120)^2\}](P/B_0)^3 + [\{-1.3371 + 2.5566(w/120) - 1.8194(w/120)^2\}(t/d)^3 + \{6.8885 - 12.3107(w/120) + 8.8723(w/120)^2\}(t/d)^2 + \{-12.5142 + 20.9008(w/120) - 15.1267(w/120)^2\}(t/d) + \{6.5631 - 9.2754(w/120) + 6.9223(w/120)^2\}](P/B_0)^2 + [\{0.1994 - 0.4645(w/120) + 0.3351(w/120)^2\}(t/d)^3 + \{-1.0977 + 2.3260(w/120) - 1.6283(w/120)^2\}(t/d)^2 + \{1.7329 - 3.2528(w/120) + 2.3300(w/120)^2\}(t/d) + \{-0.9846 + 1.6253(w/120) - 1.1807(w/120)^2\}](P/B_0). \tag{7}$$

The prying action force is $p = 0$ when the coefficient obtained by Eqs. (6) and (7) is negative. However, $p = 0.3333$ when the coefficient exceeds 0.3333.

4.2.3 T-flange stress inspection

(1) The bending stress check of the T-flange shall be performed at the center position of the bolt and the joint position with the T-web.

(2) For the calculation of the T-flange bending moment, the bolt axial force acts as a concentration force on the bolt center, whereas the prying action force can be calculated as the concentration force acting on the flange edge.

(3) The bending stress of the T-flange should satisfy Eqs. (8) and (9)

$$\sigma_{bf} = \frac{M_b}{W_b} \leq \sigma_a \tag{8}$$

$$\sigma_{wf} = \frac{M_w}{W_w} \leq \sigma_a \tag{9}$$

a) where the working force P is greater than or equal to the pre-tension axial force on the bolt B_0:

$$\sigma_{\mathrm{wf}} = \frac{\mathrm{M_w}}{\mathrm{W_w}} = \frac{6(\mathrm{ap} - \mathrm{b})\mathrm{P}}{\mathrm{wt}^2} \tag{10}$$

$$\sigma_{bf} = \frac{M_b}{W_b} = \frac{6apP}{w_n t^2} \tag{11}$$

b) where the working force P is less than the pre-tension axial force on the bolt B_0

$$\sigma_{wf} = \frac{M_w}{W_w} = \frac{6\left(ap\frac{B_0}{P} - b\right)P}{wt^2} \tag{12}$$

$$\sigma_{bf} = \frac{M_b}{W_b} = \frac{6a\{(p + 0.25\}\frac{B_0}{P} - 0.25\}P}{w_n t^2} \tag{13}$$

4.3 Design results for the joint

The yield strength of the end plate steel is 340 N/mm^2. Using JSS IV 05-2004, the tensile stress of the bolt against the design load and the bending stress of the end plate were calculated and compared with the allowable stresses and forces. Fig. 8 shows the results, which are the calculated key values for the 14 cases: the two cases of pre-tension axial force (B_0) (75% and 50% of the bolt yield axial force (B_y)) and the seven cases of end plate thickness (t), i.e., 30, 40, 50, 55, 60, 65 and 70mm, for each of the pre-tension axial forces on the bolts. The axial forces on the bolts were calculated from this prying action force coefficient (p), which was calculated from the criteria in JSS IV 05-2004.

According to the results, the thickness of the end plate should be 64 mm and more when the pre-tension axial force on the bolts is 75% of their axial yield strength and 52 mm and more when it is 50% (Fig. 8). The end plate is the first part to reach the allowable stress (in the corner near the flange of the post), and it can be seen that there is a enough margin for the bolt strength. This means that a bolt reaches the allowable tensile stress, σ_{Ba}, in case the end-plate thickness is 47 mm when the pre-tension axial force on the bolts is 75% of their axial yield strength, and that all bolts are within the allowable tensile stress regardless of thickness of the end plates when it is 50%. Furthermore, as the pre-tension axial force of the bolt decreases, the bolt axial force (B) corresponding to the same design load decreases.

5. New design method using the elastoplastic finite element method (LS-DYNA)

5.1 Numerical analysis of the bolted tensile joint using LS-DYNA

Numerical calculation using the finite element method was performed to analyze the behavior of the tower crane mast joint in detail. To perform the massive parallel calculations, we used the supercomputer system of University of Hyogo.

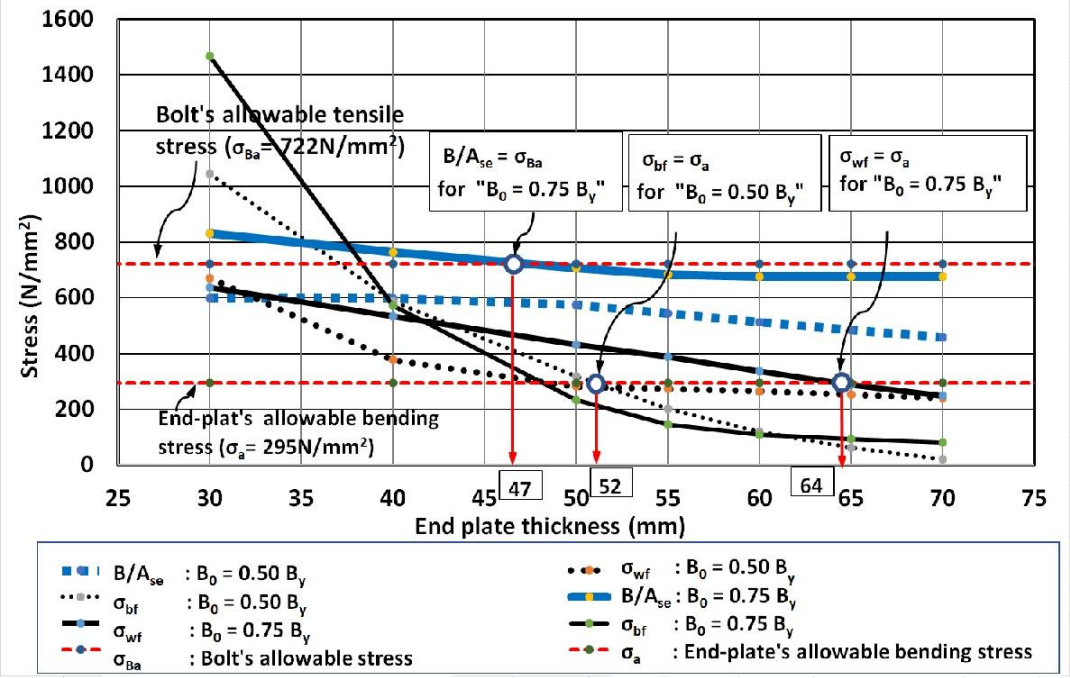

Fig. 8 Verification of bolt tensile stresses and end-plate bending stresses

5.1.1 Numerical calculation method

For the calculation, we used LS-DYNA R 9.2.0 _ Rev. 119543, which was developed by LSTC. This software employs an explicit scheme, and it can calculate large-scale problems at high speed. It is suitable for analyzing nonlinear problems, including those involving large deformations, and it is possible to stably calculate buckling and fracture phenomena. Therefore, the collapse of a structure and the ultimate proof stress can be accurately evaluated. Furthermore, given that the software can accurately analyze the contact state between parts by using its own contact algorithm, it can accurately model and evaluate the assembled structure by bolt joining. Therefore, this software should be suitable for the numerical analysis in this research. The recent good application examples of this software refer to Ushio et al. (2019) on a dynamic FEM analysis for the tower crane mast joint same as the one described in this paper and Mizushima et al. (2018) for full-scale steel structures .

5.1.2 Modeling of the end plate–type tensile bolted joint

(1) Model overview

The in-situ joint of the tower crane mast was modeled by cutting at locations 450 mm above and below the joining face. All members were modeled as solid elements for which a 2.5 mm mesh size was decided based on one side, and the minimum plate thickness of 10 mm was divided into three or more parts. For the shape of the joint, H-shaped steel posts (H-305 × 305 × 10 × 15), large-diameter M 45 hexagon bolts, and end plates with thicknesses of 30, 50, and 70 mm were prepared. The number of elements in the models was from 930,000 to 1,400,000, and the number of nodes was from 1 to 1.5 million. Figure 9 schematizes the model. Figure 10 shows an image of the mesh size.

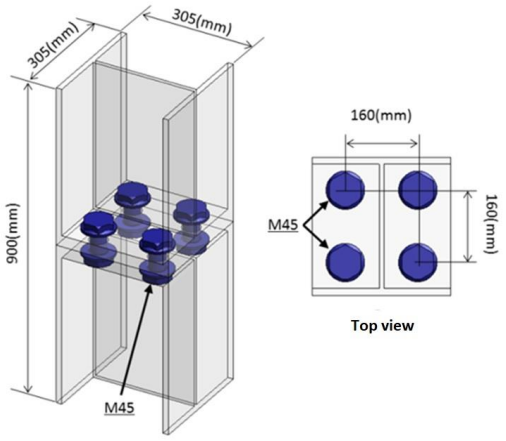

Fig. 9 Outline of the model

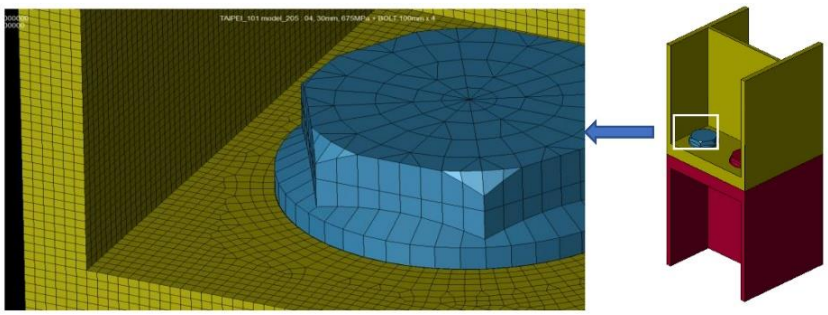

Fig. 10 Mesh size for modeling

(2) Material model

An elastoplastic material model (* MAT_PLASTIC_KINEMATIC) (LS-DYNA KUM I, Ⅱ) that is included in the software and considers kinematic hardening was used for the modeling of material properties. In this model, both kinematic ($\beta = 0$) and isotropic hardening ($\beta = 1$) can be obtained by setting the hardening parameter β ($0 < \beta < 1$). In this analysis, kinematic hardening ($\beta = 0$) was used.

It is also possible to consider the fracture behavior after yielding, which is used for modeling general metal materials, composite materials, plastics, and similar materials. Although the influence of the strain rate can be considered, no shock load was applied in this analysis; thus, it was excluded. Furthermore, the breakage of elements was not considered. Table 3 lists the properties of the materials used.

(3) Contact condition

The bolted joint connecting members were modeled in as a real situation as possible by defining the contact conditions on the surface between the end plates welded to the upper and lower posts and between the washer and end plate. The contact conditions are controlled by the "constrained method" using the contact determination function (*CONTACT_AUTOMATIC_ SURFACE_TO_SURFACE) (LS-DYNA KUM I, II) included in the software. The friction coefficient for these contact surfaces was assumed as 0.1.

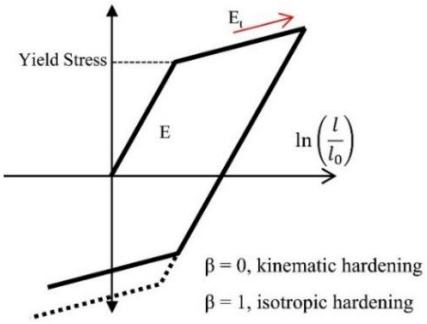

Fig. 11 Hardening of the elastoplastic material

Table 3 Material properties

	Young's Modulus (E)	Hardening (E_t)	Density	Poisson's Ratio	Yield Strength
	(MPa)	(MPa)	(ton/mm^3)		(MPa)
H-shape & plate	206,000	0.01E	7.89E−09	0.3	340
Bolt	210,000	0.01E	7.89E−09	0.3	900

(4) Loading conditions

By completely fixing the lower end of the mast site joint, force is applied with a displacement of +5 mm at the upper end in the tensile direction. To suppress the impact load during the time between the start and end of loading in each loading step, the slopes of the load curve at the start and end are made gentle. Figure 12 shows the loading condition, and Figure 13 shows the loading displacement curve for suppressing the impact load.

5.1.3 Joint types for analysis

The mast site joints of a tower crane that is generally used for steel high-rise buildings were chosen as the models for analysis. We chose to analyze the same type of tower crane that suffered from collapse during the previously mentioned earthquake. The key members of the joints are composed of H305 × 305 × 10 × 15 (σ_y = 340 N/mm^2) as the post member and M45 (Class 10.9) bolts. Furthermore, the seven analysis model cases shown in Table 4 were chosen using the following three items as parameters and were analyzed by LS-DYNA for each case. The allowable tension strength of each joint was then calculated according to the crane structural standard (JIS B 8821 (2013)). When selecting the joint types for analysis, the eccentric end plate–type tensile bolted joint with six bolts, which is difficult to design with high precision using the conventional design method described in Section 4, was also added to the analysis target:

(1) Thicknesses of end plates (30, 50, and 70 mm)

(2) Number of bolts (two type of joints shown in Fig. 14)

(3) Pre-tension axial force on bolts (rates of bolt yield strength: 50% and 75%)

For example, in the case of H4-3075, the analyzed model is named as follows: sectional shape of the post (H-shaped steel), 4; number of bolts, 30; thickness of the end plate (30 mm), 75; pre-tension force on bolts (% to bolt yield strength: 75%)

Figure 14 shows the arrangements of bolts and stiffeners in four- and six-bolt joints.

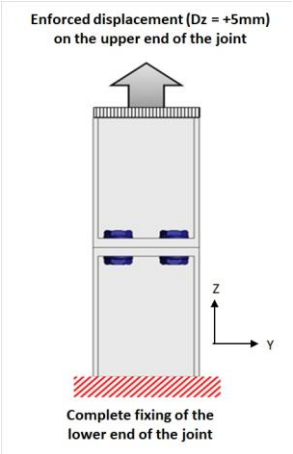

Fig. 12 Loading condition

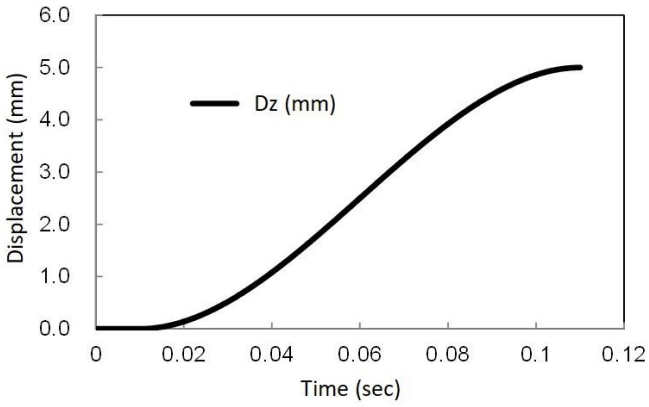

Fig. 13 Displacement curve to suppress the impact load

Table 4 Seven cases for analysis models

	1	2	3	4	5	6	7
Name	H4-3075	H4-3050	H4-5075	H4-5050	H4-7075	H4-7050	H6-5075
Thickness	30 mm	30 mm	50 mm	50 mm	70 mm	70 mm	50 mm
No. of bolts	4	4	4	4	4	4	6
Pre-tension	75%	50%	75%	50%	75%	50%	75%

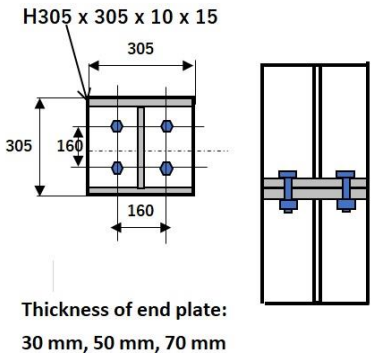

(a) Four-bolts joint
(same as the joint in the above Taiwan case)

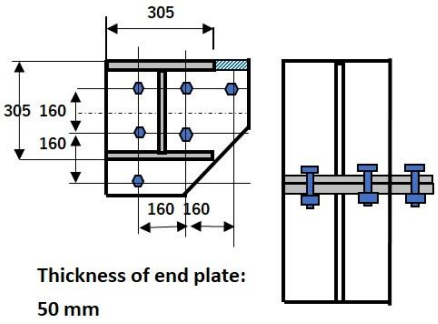

(b) Six-bolts joint (add two bolts)

Fig. 14 Joint detail of the models for analysis

5.2 Analysis results used for the joint design

As specified in JSS IV 05-2004, the bolt axial force considering the prying action force and bending stress in the end plate are verified for joint design to ensure that they are within the allowable values (JIS B 8821 (2013)). From the analysis result data obtained by LS-DYNA, three types of numerical data listed below are extracted for each loading step. The parts of the joint are meshed as finely as possible to solid

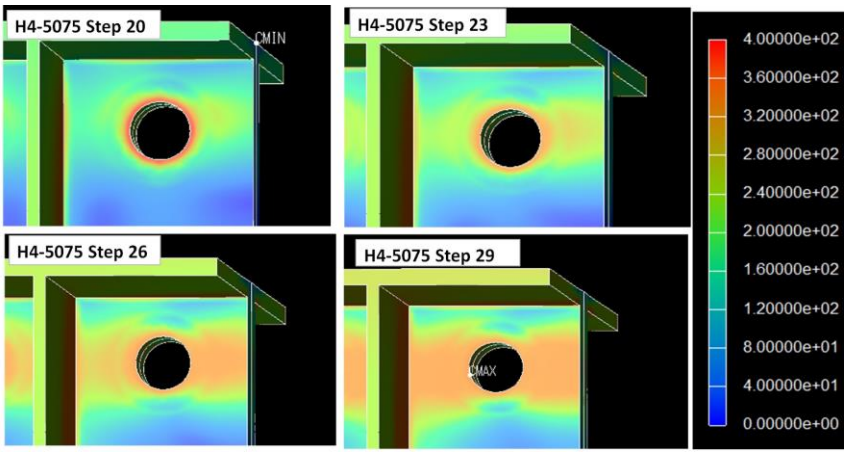

Fig. 15 Contour diagram of the von Mises stress in the end plates of analyzed model H4-5075

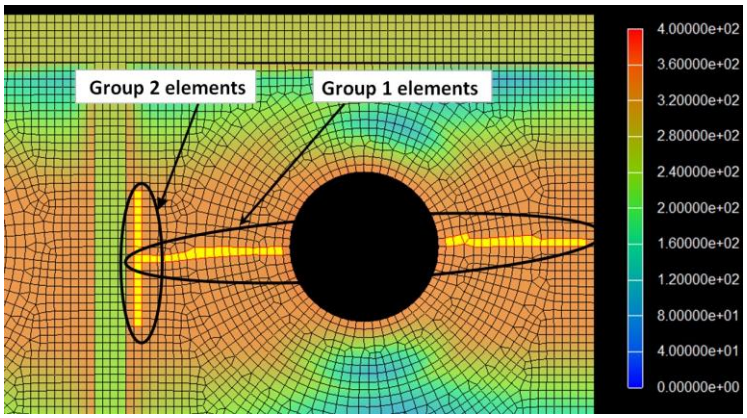

Fig. 16 Solid element groups with high von Mises stresses in the end plate

elements, and a more realistic situation is reproduced. Therefore, it should be assumed that the following numerical data can be calculated with high accuracy:

(1) Axial tensile forces on the bolts (section force)
(2) Tensile forces on the joint (tensile force acting on post)
(3) Von Mises stresses in the end plate solid elements.

Items 1 and 2 above were calculated using the functions incorporated in LS - DYNA, but it was difficult to calculate item 3. For this item, in the case wherein the maximal value among the von Mises stresses of all solid end plate elements is compared with the allowable bending stresses of the end plates in this joint design, such an allowable stress design method is impractical because some elements may have high stress owing to stress concentrations. After examining the distribution of von Mises stresses in the end plates, it was concluded that the solid element groups with high von Mises stress values should be determined (Fig. 16). It was also concluded that the average values of the stresses in the solid elements of each group should be calculated, and the highest of the average values should be taken as the design stress of the end plate. The elements at the corners of the H-shaped steel post and the edge of the plate, which are subject to concentrated

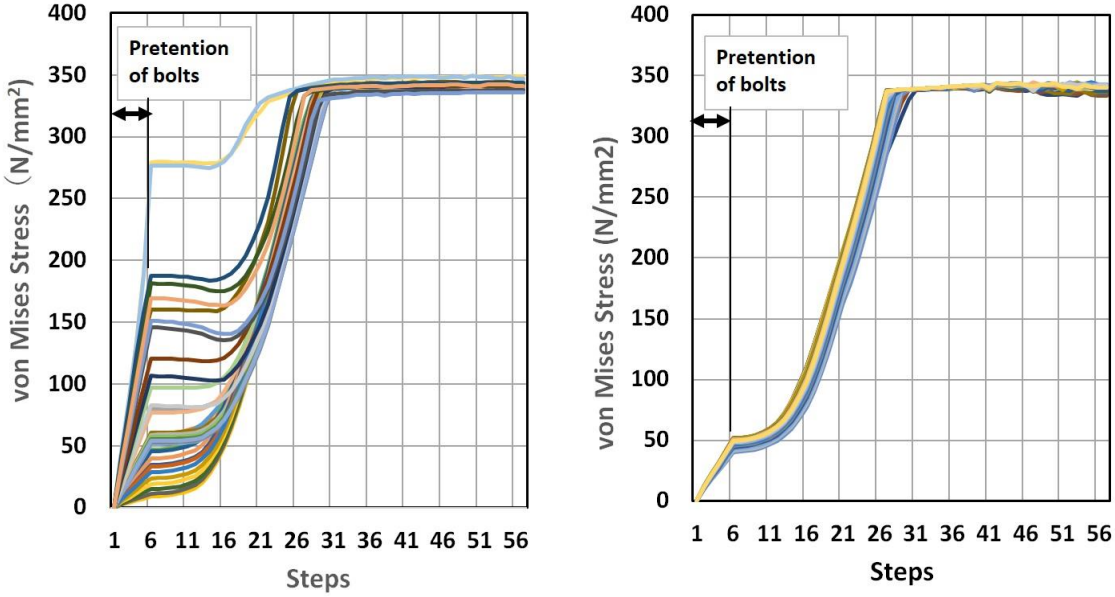

(a) von Mises Stress of Group 1 elements (b) von Mises Stress of Group 2 elements

Fig. 17 Von Mises stresses of the elements of critical groups 1 and 2 at each loading step

stress, were excluded. In this determination, the von Mises stresses in the elements at the surface of the end plate during loading steps 20, 23, 26, and 29 were observed using contour diagrams. This was performed to visualize the size of the stresses considering that the stress in a surface element of the end plate is dominated by bending in the out-of-plane direction. Figure 15 shows the contour diagram for analyzed model H4-5075 as an example.

Figure 17 shows the transition of the von Mises stress in each element for the loading steps for the two end plate element groups marked in Fig. 15. Furthermore, using the above method, the stress transition values for the end plate design of the seven analyzed models are shown in Figure 18. This design stress varies considerably depending on the thickness of the end plate, and there is little influence caused by the increase in the bolt pre-tension axial force and by the number of bolts.

5.3 New design pattern to obtain the allowable tensile strength of the joints

For the joints listed in Table 4, Figs. 19-22 illustrate how to obtain the design tensile strength of the end plate-type bolted tensile joint using the analysis results calculated by LS-DYNA, according to JIS B 8821(2013).

The design procedure is specifically explained in Fig. 19(a). This figure shows the three transition curves of the following stresses and forces (described in Section 5.2) for each loading step obtained from the LS-DYNA analysis:

(1) Axial tensile forces on the bolts (section force)
(2) Tensile forces on the joint (tensile force acting on post)
(3) Von Mises stresses in the end plate solid elements

The left vertical axis of the graph represents the von Mises stress (N/mm^2), whereas the right

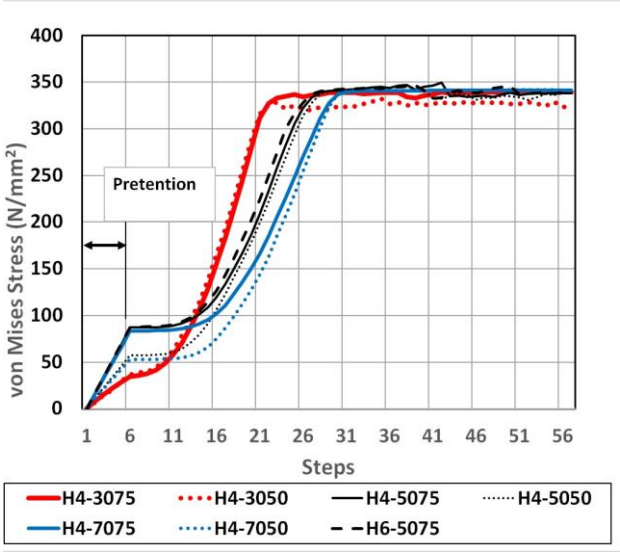

Fig. 18 Critical von Mises stresses of the end plates of the seven analyzed models to be used for design

vertical axis represents the tensile force (kN) corresponding to the values of the bolt axial forces and the tensile load on the joint for one bolt. Furthermore, the allowable bending stress (σ_a) of the end plate and the allowable tensile strength (B_a) of the bolt specified in JIS B 8821 (2013) are indicated by horizontal dotted lines. The loading steps at which the axial force of the bolt and the design von Mises stress of the end plate reach their allowance values (stipulated in JIS B 8821 (2013)) are obtained from the graphs. The steps are indicated by the point of intersection between the dotted line of B_a and the transition curve of the bolt axial force, and the point of intersection between the dotted line of σ_a and the transition curve of the design von Mises stress of the end plate.

The tensile load at the loading step at which one of the two points first reaches the allowable values, is used as the allowable tensile strength of the bolted tension joint. Given that the graph shows the loading force for one bolt, the allowable tensile strength of the joint is calculated by multiplying the number of bolts by the value obtained from the graph. Figure 19(b) shows the design results when the pre-tension bolt axial force is 50 percent of the bolt yield strength.

Using this design method and the analysis results calculated by LS-DYNA, it is possible to design end plate type bolted tensile joints even if they have complicated shapes. Moreover, the joint design can consider the bolt pre-tension axial force.

For the remaining five models shown in Table 4, the design results obtained by this method are shown in Figs. 20 to 22. For the easy comparison of the graphs for the cases of joints with four bolts, two cases with different bolt pre-tension axial forces are shown side by side for each plate thickness.

Table 5 summarizes the design results, such as the allowable tensile strengths of the joint models in Table 4:

Using the abovementioned method with LS-DYNA, even for eccentric-bolted tensile joints in which the post members are angle shaped or rectangular tube steel, engineers can design the joints to a more accurate level according to JIS B 8821 (2013).

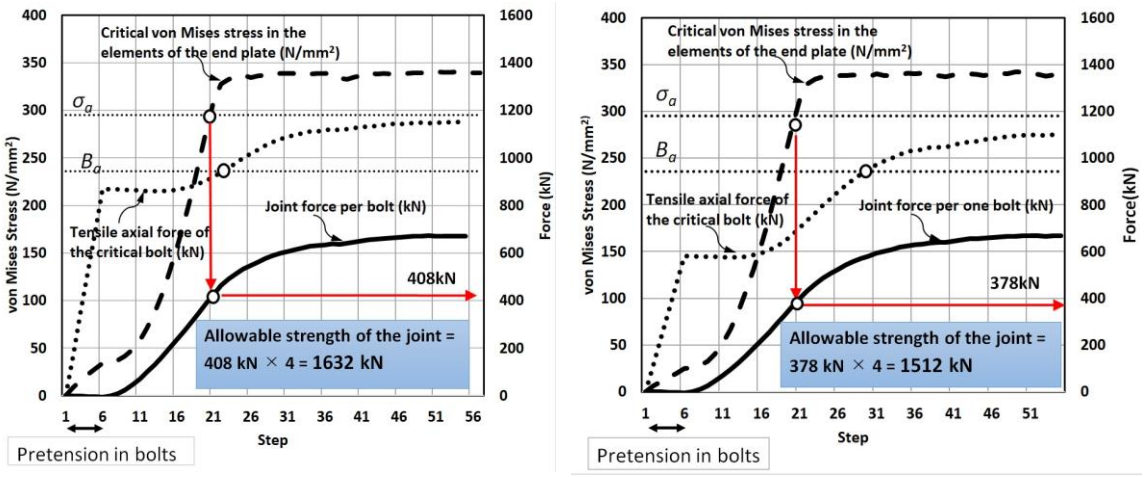

(a) H4-3075 (b) H4-3050

Fig. 19 Calculation of the allowable strength of joint models H4-3075 and H4-3050

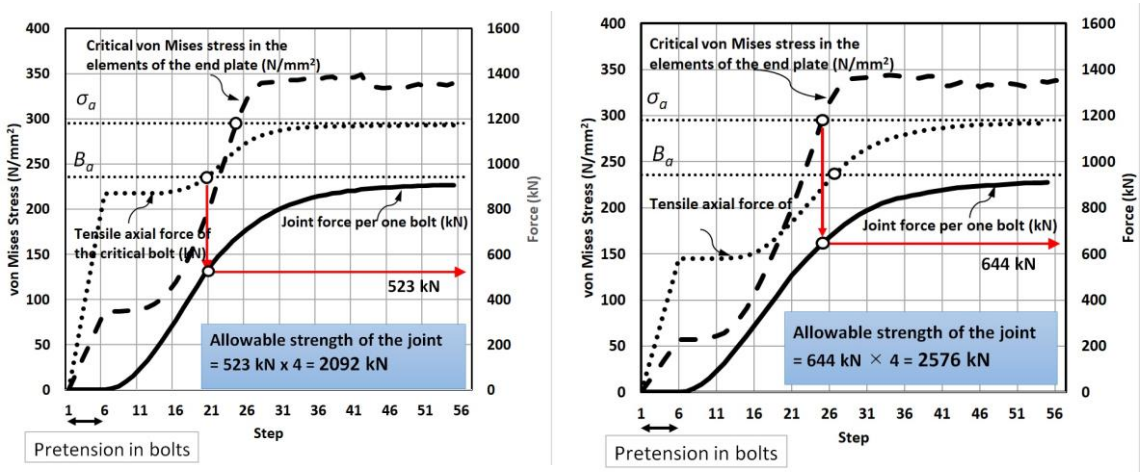

(a) H4-5075 (b)H4-5050

Fig. 20 Calculation of the allowable strength of joint models H4-5075 and H4-5050

6. Advantages of the new design method versus the conventional method

Based on the design results shown in Fig. 8 and Figs. 19-22, the advantages of the new design method using LS-DYNA compared with the conventional design method based on JSS IV 05-2004 are described below:

(1) Accuracy of the calculation of end plate thickness

Table 6 shows the thickness of the end plate calculated by both design methods. Although there is no significant difference between the obtained thicknesses of the end plates, the design result obtained using LS - DYNA is somewhat more economical (smaller plate thickness) and reliable because engineers can accurately grasp the stress situation of each part of the joint.

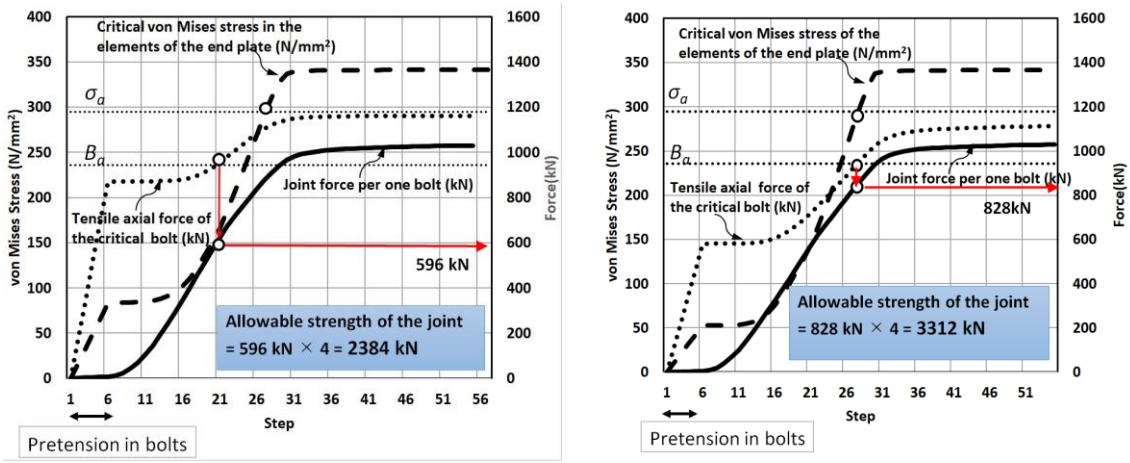

(a) H4-7075 (b) H4-7050

Fig. 21 Calculation of the allowable strength of joint models H4-7075 and H4-7050

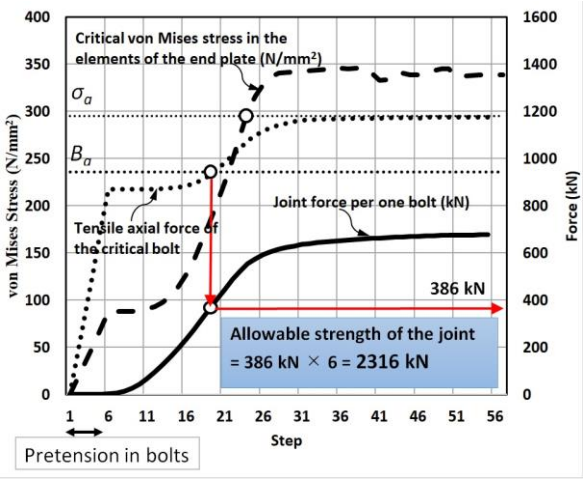

Fig. 22 Calculation of the allowable strength of joint model H6-5075

Table 5 Allowable strengths of the joint models and failure pattern

	Joint Type	Number of bolts	EPL thickness (mm)	Pre-tension of each Bolt*1	Allowable tensile strength of the joint (kN)	Failure pattern (first part to reach its allowable stress)
H4-3075	1	4	30	75%	1632	End plate
H4-3050	1	4	30	50%	1512	End plate
H4-5075	1	4	50	75%	2092	Bolts
H4-5050	1	4	50	50%	2576	End plate
H4-7075	1	4	70	75%	2384	Bolts
H4-7050	1	4	70	50%	3312	Bolts
H6-5075	2	6	50	75%	2316	Bolts

*1: Rates of yield strength of the bolt (1170kN = 0.9kN/mm^2 x 1301mm2)

Table 6 Comparison of the design method results

Design method	Bolt's pre-tension	No. of bolts	Thickness of the end plate (mm)	First Part to reach allowable stress
Conventional method (JSS IV 05-2004)	$B_0 = 0.75B_y$	4	64	End plate
	$B_0 = 0.50B_y$	4	52	End plate
Proposed method (Elastoplastic FEM (LS-DYNA))	$B_0 = 0.75B_y$	4	55*2	Bolt
	$B_0 = 0.50B_y$	4	45*2	End plate (close to the bolt)

* 1 Adopted bolt: size M 45, material JIS B 1051, strength classification 10.9
* 2 Calculated by the proportional distribution from the results of the analyzed models with an end plate thickness of 70 mm (H4-7075 and H4-7050)

(2) Accurate understanding of the fracture pattern of joints

In the conventional design method based on JSS IV 05-2004, Figure 8 shows that for H4-5075 and H4-5050 with different pre-tension axial forces on the bolts, the end plate first reached the allowable stress, and the bolt still had a room to reach the allowable stress. On the contrary, with the new design method using LS-DYNA, as shown in Fig.20 (a), the bolt first reached the allowable stress in the H4-5075 model. The reason for the difference in the fracture pattern seems to be the difference of accuracy of the results calculated by two methods. For example, the prying action force on the bolts calculated according to the JSS IV-2004 criteria is underestimated when the end plate is thicker as explained in Fig. 23 which shows the bolt tension force against end plate thicknesses calculated by the conventional and the proposed methods under the design load of 537kN per bolt for comparison. In particular, for end plate-type bolted tensile joints, it is normally required for the structural design to avoid the brittle fracture that occurs in bolts. Therefore, using the new design method, engineers can accurately grasp the fracture pattern of the joint, find measures to prevent brittle fracture, and produce flexible designs.

(3) Design considering construction conditions

The conventional design method calculates the tensile stress in the bolt and the bending stress in the end plate based on the design load and compares these stresses with the allowable values. By contrast, the new design method calculates the various stresses and forces at the loading steps from the introduction of the pre-tension axial force on the bolt to the loading on the joint. Therefore, according to the new method, it is possible to design joints in consideration of construction conditions such as the magnitude and variation of the pre-tension axial forces to be applied to the bolts at the time of construction as well as the fabrication and construction accuracy of the joints, etc. Figures 20 and 21 show that when the thickness of the end plate is thicker (50 and 70 mm), the allowable tensile strength of the joint increases by 23% at 50 mm of the thickness of the end plate and by 39% at 70 mm by lowering the pre-tension axial force on the bolt from 75% to 50% of the bolt yield strength.

(4) Application to complicated joints

Regarding the joints (Figs. 3(b) and (c)) for which the modeling to T-joints is difficult, the conventional design method cannot be applied for the accurate design of the joints. Even if it is applied, the designed joints will be uneconomical joints with a high safety factor. Therefore, a highly accurate design can be created using the new method. Figure 22 shows the design results of the joint (H6-5075) reinforced by two additional bolts; this joint is difficult to model as a T-joint. The results obtained using the new method show that any eccentricity causes each bolt in the joint

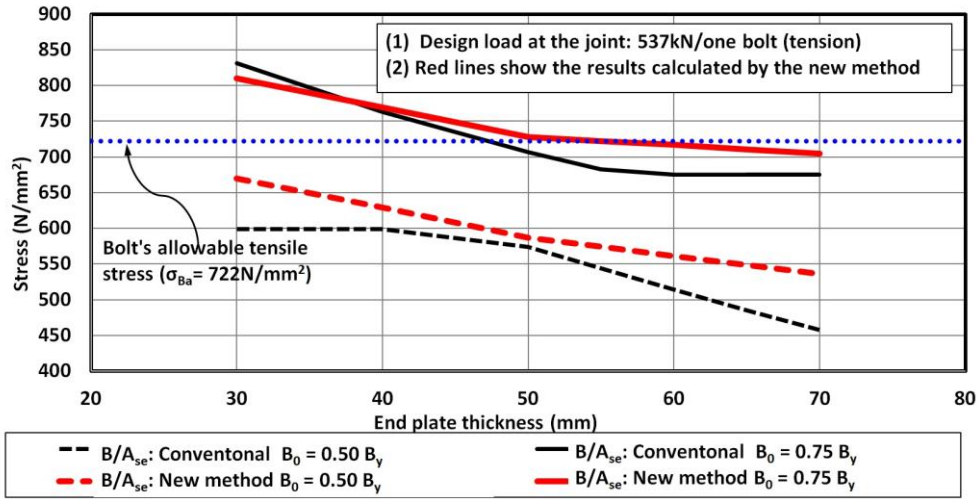

Fig. 23 Tension forces of bolts calculated using the conventional and new proposed methods

to have a biased tension force such that the allowable joint force must be determined based on the bolt with the largest tension load. As such the joint is not efficient. This problem could be solved by changing the critical bolts to the ones having larger diameter. This proposed design method can thus overcome the problems associated with such joint design.

7. Conclusion

A new design method that uses the static elastoplastic finite element method (LS-DYNA) has been described for an end plate-type tensile bolted joint, which is generally applied at the site bolt joints of a tower crane mast. For the on-site joints of the tower crane mast that are assembled on site, the design must satisfy all the relevant requirements, including ease of assembly/dismantling work in the field, safe collapse pattern (avoid breakage from bolts, etc.) and strength. To this end, a minimal element FEM analysis model must be analyzed using a supercomputer and the highly reproducible analysis results must be directly used in the design. By applying this method to, for example, a complex eccentric-tension bolt joint, the engineers can realize a detailed design in consideration of many parameters such as the enlargement of diameter of the bolts in response to a larger load in the joint, proper pre-tension of bolts, optimization of the bolt layout. Such designed joints, however, require the application of sufficient quality control during construction as usual.

The design method proposed in this paper makes it possible to design the joint that achieves both workability and strength. In addition, we are confident that this new design method will help improve the earthquake resistance of tower cranes. Furthermore, this method is applicable not only to tower crane masts but also to bolted tension joints in all structures.

Acknowledgments

The authors would like to thank Enago (www.enago.jp) for the English language review.

References

AIJ Recommendation (2012), Recommendation for Design of Connections in Steel Structure, (revised in March 2012), Architectural Institute of Japan, Japan.

ISO11031 (2016), Cranes-Principles for seismically resistant design, International Standard Organization, , Japan.

JCAS1101(2008), Seismic Design Guideline for Cranes, the Japan Crane Association (JCA), Japan.

JIS B1082 (2009), Stress Area and bearing area for threaded fasteners, Japanese Standards Association, Japan.

JIS B8821 (2013), Calculation standards for steel structures of cranes, Japanese Standards Association, Japan.

JIS B8831 (2004), Cranes-Design Principles for loads and load combination, Japanese Standards Association, Japan.

JSS IV 05-2004, Recommendation for design of High Strength Tensile Bolted Connections for Steel Bridges, (revised in August 2004), Japanese Society of Steel Construction (JSSC), Japan.

LS-DYNA KUM I (2016), LS-DYNA Keyword User's Manual Volume I (LS--DYNA R8.0), JSOL Corporation, Japan.

LS-DYNA KUM II (2016), LS-DYNA Keyword User's Manual Volume II (LS-DYNA R8.0), JSOL Corporation, Japan.

Ai, B., Yang, J. and Pei, Z. (2013), "Seismic response analysis of tower crane in consideration of the building-crane interaction", *Appl. Mech. Mater.,* **353-356**, 1981-1985. https://doi.org/10.4028/www.scientific.net/AMM.353-356.1981.

Kobayashi, N. (2017), "ISO1131: Craines-Principles for seismically resistant design and seismic design", *J. Japan Crane Assoc.*, **55**(635), 4-10

Loh C.H. Loh, Tsai K.C., Chung L.L. and Yeh C.H. (2003), "Reconnaissance report on the 31 March 2002 earthquake on the east coast of Taiwan", *Earthq. Spectra*, **19**(3), 531-556. https://doi.org/10.1193/1.1598438.

Mizushima.Y., Mukai. Y., Namba. H., Taga. K. and Saruwatari. T., (2018), "Super detailed FEM simulations for full-scale steel structure with fatal rupture at joints between members – Shaking table test of full-scale steel frame structure to estimate influence of cumulative damage by multiple strong motion: Part 1", *Japan Architectural Review,* **1**(1), 96-108. https://doi.org/10.1002/2475-8876.10016.

Takanashi, S. (2005), "Damage to the cranes and seismic design", *J. Reality Eng. Assoc. Japan (REAJ)*, **27**(8), (series No. 148). https://doi.org/10.1061/40834(238)105.

Takanashi, S., Adachi, H. and Nakanishi, M. (2007), "Study on the seismic performance of the tower crane for construction", *Architectural Institute of Japan Technical Report*, **13**(26), 415-420.

Ushio, Y., Saruwatari, S. and Nagano, Y. (2019), "Elastoplastic FEM analysis of earthquake response for the field-bolt joints of a tower crane mast", *Adv. Comput. Design*, **4**(1), 53-72. https://doi.org/10.12989/acd.2019.4.1.053.

Ushio, Y., Okano, M. and Nagano, Y. (2017), "The earthquake response of climbing-type tower cranes installed in high-rise buildings in consideration of various situation under construction", *Proceedings of 16th World conference on Earthquake Engineering,* Santiago, Chile. January.

Yang, J., Park, J., Kim, H. and Back, M. (2013), "A prying action force and contact force estimation model for a T-stub connection with high-strength bolts", *J. Asian Architect. Build. Eng.*, **12**(2), 309-316. https://doi.org/10.3130/jaabe.12.309.

Wang, X., Luo, Y., Qiang, X. and Liu, X. (2015), "Review on high strength steel bolted end-plate connections", *Appl. Mech. Mater.,* **744-746**, 265-273. https://doi.org/10.4028/www.scientific.net/AMM.744-746.265.

Appendix

Parameters

P : Tensile force acting on one bolt under design load (kN)
B_0 : Pre-tension axial force of a bolt (kN)
w : Width of a T-flange per one bolt (mm) (Fig. 3-2)
w_n : Net width of a T-flange per one bolt (mm)
t : Thickness of an end plate (mm)
B : Axial force of a bolt (N)
B_y : Yield strength of a bolt (kN)
d : Nominal diameter of a bolt (mm)
A_{se} : Effective cross-sectional area of the threaded portion of a bolt (mm^2)
p : Prying action force coefficient
σ_{Bu} : Ultimate tensile strength of bolts (N/mm^2)
σ_{Ba} : Allowable tensile stress of bolts (N/mm^2)
$\sigma_{B\,y}$: Yield strength of bolts (N/mm^2)
σ_{bf} : Bending stress of a T-flange at a bolt location (N/mm^2)
σ_{wf} : Bending stress of a T-flange at a T-web location (N/mm^2)
σ_{vm} : von Mises stress of end plate (N/mm^2)
σ_a : Allowable bending stress of a T-flange steel material (N/mm^2)
M_b : Bending moment of a T-flange at a bolt location (N・mm)
M_w : Bending moment of a T-flange at a T-web location (N・mm)
W_b : Section modulus of a T-flange at a bolt location
W_w : Section modulus of a T-flange at a T-web location